



# Nonmeningothelial Dural-Based Lesions: A Histopathological Analysis

Pooja K. Gajaria<sup>1</sup> Asha S. Shenoy<sup>1</sup> Naina A. Goel<sup>1</sup>

<sup>1</sup>Department of Pathology, Seth G. S. Medical College and K. E. M. Hospital, Mumbai, Maharashtra, India

Address for correspondence Asha S. Shenoy, MD, 301, Arihant, 613-B, 15th Road, Khar, Mumbai, 400052, Maharashtra, India (e-mail: shenoyasha@yahoo.co.in).

Asian J Neurosurg 2023;18:484–491.

## Abstract

**Introduction** We report 30 cases of nonmeningothelial dural-based lesions encountered during a 3-year study period.

**Materials and Methods** We retrospectively reviewed pathology records of patients operated for extra-axial, dural-based lesions during the years 2016 to 2018 and included nonmeningothelial lesions as a part of this study.

**Results** Among the 3,243 neurosurgical specimens for histopathologic examination, only 30 (0.93%) were “nonmeningothelial dural-based lesions.” Six (20%) patients were in the pediatric age group. Pathologic assessment identified 13 cases of solitary fibrous tumor/hemangiopericytoma (43.3%) and 7 cases of Ewing’s sarcoma/primitive neuroectodermal tumor (23.3%). Two cases (6.7%) were of metastasis. Other lesions included a single case each of non-Hodgkin’s lymphoma, undifferentiated sarcoma, solitary plasmacytoma, and granulocytic sarcoma. Nonneoplastic lesions included two cases each of Rosai–Dorfman disease and nonspecific inflammatory lesions.

**Conclusion** Nonmeningothelial dural-based lesions being rare, thorough examination of morphological features is a must by the pathologist, to arrive at the accurate diagnosis. Ancillary tests, if required, should be employed in the context of the morphologic picture.

## Keywords

- ▶ dura
- ▶ extra-axial
- ▶ infectious
- ▶ neoplastic
- ▶ nonmeningothelial

## Introduction

Meningiomas are common mass lesions that affect the dura, and account for 36% of all brain tumors.<sup>1</sup> Tumefactive nonmeningothelial lesions affecting the dura include both nonneoplastic as well as neoplastic entities. Neurosarcoidosis, Rosai–Dorfman disease (RDD), and infective granulomas are some of the nonneoplastic lesions known to affect the dura. Neoplastic lesions include solitary fibrous tumor (SFT)/hemangiopericytoma (HPC), metastasis, lymphomas, plasmacytomas, melanocytic tumors, Ewing’s sarcoma (ES)/primitive neuroectodermal tumor (PNET), and a variety of

other mesenchymal tumors.<sup>1</sup> Some of these lesions are commonly reported as soft-tissue masses at other sites in the body; however, their occurrence in the dura is rare. These nonmeningothelial lesions show an assorted variety of pathologies. Most of these are reported as single case reports in the literature.

Some of the lesions cannot be typified on radiology and pathologic assessment remains the gold standard for accurate diagnosis. Many of these have overlapping morphological characteristics, and hence the pathologist is required to have a thorough knowledge of the peculiar features on

article published online  
September 22, 2023

DOI <https://doi.org/10.1055/s-0043-1771315>.  
ISSN 2248-9614.

© 2023. Asian Congress of Neurological Surgeons. All rights reserved.

This is an open access article published by Thieme under the terms of the Creative Commons Attribution-NonDerivative-NonCommercial-License, permitting copying and reproduction so long as the original work is given appropriate credit. Contents may not be used for commercial purposes, or adapted, remixed, transformed or built upon. (<https://creativecommons.org/licenses/by-nc-nd/4.0/>)

Thieme Medical and Scientific Publishers Pvt. Ltd., A-12, 2nd Floor, Sector 2, Noida-201301 UP, India

morphology. Ancillary studies should be ordered keeping in mind the histomorphologic characteristics to arrive at a clinically helpful diagnosis. This prompted us to study the spectrum of the nonmeningeothelial dural-based lesions that presented to our institute, over a period of 3 years. In this study, we discuss the approach followed for diagnosing these nonmeningeothelial dural-based masses. To the best of our knowledge, ours is the largest study to be reported, compiling a wide variety of these lesions.

### Materials and Methods

The retrospective observational study was conducted after permission from the Institutional Ethics Review Board. This is a single institutional study, and cases were selected from the pathology records of patients operated for extra-axial, dural-based lesions, at our tertiary care center over a period of 3 years (2016–2018). Inclusion criteria were the presence of a dural-based lesion on magnetic resonance imaging (MRI) and intraoperative findings confirming the same. The archived hematoxylin and eosin–stained as well as immunohistochemistry (IHC) slides were reviewed. Some of the neoplastic lesions were reclassified according to the 2016 World Health Organization (WHO) classification of central nervous system (CNS) tumors. Accordingly, all cases reported as SFT or HPC were clubbed into a single entity and were graded as follows:

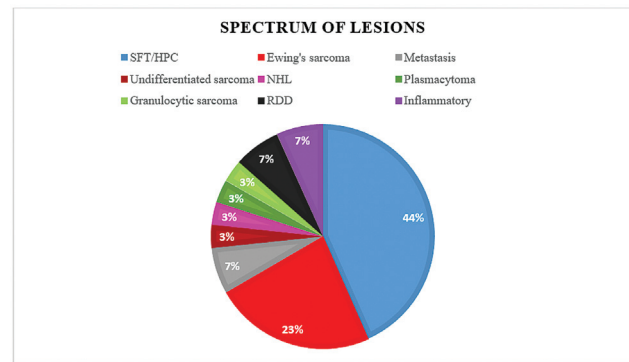
- Grade I SFT/HPC: Hypocellular, collagenized tumor with SFT phenotype.
  - Grade II SFT/HPC: Intermediate in morphology with less than 5 mitoses per 10 high-power fields (hpf).
  - Grade III SFT/HPC: Densely cellular HPC-like phenotype with more than 5 mitoses per 10 hpf.
- Positivity for Ki-67 IHC was noted in the hot-spots, and an average of 10 hpf was given as the Ki-67 index.

### Results

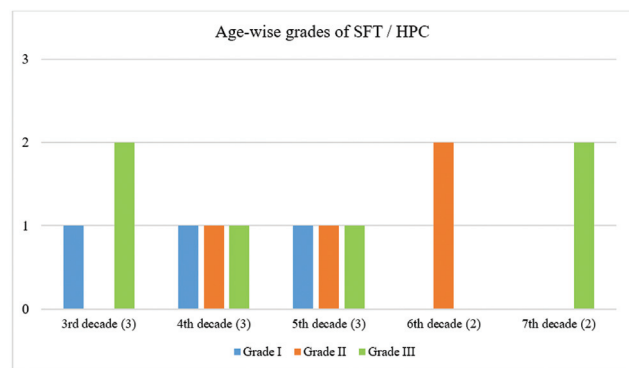
Over the 3 years, we received 3,243 neurosurgical specimens for histopathologic examination. Among these, only 30 (0.93%) were “nonmeningeothelial dural-based lesions.” Six (20%) were pediatric patients (≤ 15 years of age), while the remaining 24 (80%) were adults with a mean age of 40.3 years (range: 18–64 years). The pediatric age group ranged from 5 to 15 years. Seven lesions (23.3%) were localized in the spinal region, while the rest, 23 (76.7%) were intracranial.

The spectrum of nonmeningeothelial dural lesions diagnosed on microscopic examination in our series is shown in **Graph 1**, the respective key histologic features, clinical details, and IHC panel used for neoplastic lesions are listed in **Table 1**. Twenty-six (86.7%) were neoplastic lesions and only four (13.3%) were nonneoplastic. On MRI, 20 (66.7%) cases were diagnosed as meningioma. Diagnosis on MRI and the corresponding histopathologic diagnosis are listed in **Table 2**.

Among adults, the most commonly reported neoplasm was SFT/ HPC, in 13 cases (43.3%). Of these, 46.1% (6 out of 13) were anaplastic (WHO Grade III) (**Fig. 1A–D**), 30.8% (4 out of 13) were Grade II, and 23.1% (3 out of 13) cases belonged to



**Graph 1** Spectrum of nonmeningeothelial dural-based lesions in our study.



**Graph 2** The age-wise distribution of solitary fibrous tumor/ hemangiopericytoma cases in our series.

Grade I (**Graph 2**). One case (3.3%) was a solitary dural plasmacytoma (**Fig. 1E–H**). Even with an extensive panel of IHC markers, one of the high-grade spindle cell tumors could not be further categorized and hence was labeled as undifferentiated sarcoma.

The most common lesion (83.3%) in the pediatric population was ES/PNET (**Fig. 2A–C**), while one case was a granulocytic sarcoma, in a known case of acute myeloid leukemia (AML) on treatment (**Fig. 2D–F**).

Among the two cases (6.7%) of metastasis, one was from follicular carcinoma of the thyroid gland (**Fig. 2G–I**), and the other was an undifferentiated carcinoma with unknown primary. Another rare case (3.3%) encountered in our study was non-Hodgkin's lymphoma (NHL)—anaplastic large cell lymphoma (ALCL), anaplastic lymphoma kinase (ALK)-positive (**Fig. 3A–D**), with Ki-67 index of approximately 80% (**Fig. 3E**). The patient was a known case of acquired immunodeficiency syndrome on antiretroviral therapy.

Out of the four cases of nonneoplastic dural-based lesions that presented as a mass, two cases (6.7%) were nonspecific inflammatory lesions (**Fig. 4A,B**) that did not reveal any organisms on special stains, namely Gomori methenamine silver or Ziehl–Neelsen stain (**Fig. 4C**). The other two cases (6.7%) were of RDD, which showed classic emperipolesis (**Fig. 4D,E**), further confirmed by a positive S-100p IHC (**Fig. 4F**).

**Table 1** Summary of the neoplastic lesions in our study

Diagnosis (number of cases)	Age/Age group	Site	Histologic features	Positive IHC markers	Negative IHC markers
SFT/HPC (13)	3rd–7th decade	12 - intracranial 1 - spinal	Spindle cells in fascicles and storiform pattern, elongated vesicular nuclei, eosinophilic cytoplasm, mitotic activity varied as per grade	Bcl2, CD34, vimentin	EMA, AE1/AE3, CD99
ES (7)	5–26 years	2 spinal, rest intracranial	Round blue cell tumor; brisk mitotic activity	CD99, vimentin	LCA, AE1/AE3, desmin
Metastasis (2)	5th decade	Parietal and cerebellopontine angle	1. From follicular carcinoma of thyroid 2. Carcinoma from unknown primary		
ALCL, ALK-positive (1)	40 years	L1-L2	Dyscohesive cells in sheets, round to ovoid cells with indented nuclei and 1–3 prominent nucleoli, scant to moderate cytoplasm, binucleate, and multinucleate cells, apoptotic fragments seen	LCA, CD3, CD30, ALK-1	CD20, EMA
Plasmacytoma (1)	60 years	Parietal region	Cells in sheets, round to ovoid cells, abundant eosinophilic cytoplasm, eccentrically placed nuclei, binucleate, and multinucleate cells seen	CD38, CD138, lambda	LCA, CD3, CD20, kappa
Granulocytic sarcoma (1) – known case of AML	8 years	D3-D9	Tumor cells in sheets, monocytoïd cells, moderate cytoplasm, vesicular nuclei, prominent amphophilic nucleoli	CD117	LCA, CD3, CD20
Undifferentiated sarcoma (1)	24 years	Parieto-occipital region	Spindle cell tumor in intersecting fascicles and sheets. Elongated hyperchromatic nuclei, moderate to abundant eosinophilic cytoplasm. Mitosis, necrosis, and brain invasion seen	Vimentin	S100p, GFAP, CD34, desmin, EMA, and AE1/AE3

Abbreviations: ALCL, anaplastic large cell lymphoma; ALK, anaplastic lymphoma kinase; AML, acute myeloid leukemia; EMA, epithelial membrane antigen; ES, Ewing's sarcoma; GFAP, glial fibrillary acidic protein; HPC, hemangiopericytoma; IHC, immunohistochemistry; LCA, leucocyte common antigen; SFT, solitary fibrous tumor.

Note: Parenthesis indicating the number of cases.

## Discussion

The 2016 WHO classification of CNS tumors has grouped the neoplasms affecting the meninges (other than meningiomas) under the category of “mesenchymal, nonmeningothelial tumors.” Although these comprise only a small proportion of CNS neoplasms, precise diagnosis on histopathologic examination holds importance in view of different treatment protocols and prognosis.

A search through literature revealed mostly case reports/series of individual entities of nonmeningothelial dural-based lesions. However, our study comprises a compilation of these lesions and perhaps is the largest to be reported yet. A comparison of lesions in our study with similar cases reported in literature is shown in ► **Table 3**.

These are rare lesions, with an approximate incidence of less than 1% neuropathology cases at our tertiary care center, over 3 years. Hence, diagnosis needs expertise and utmost

caution with a systematic approach to rule out similar lesions. In today's era of targeted therapy, precise diagnosis requires testing with the help of a multitude of ancillary tests. Careful evaluation of the morphology can help the pathologist choose the correct ancillary tests for a particular case.

**Graph 1** shows that the most common lesion in our series was SFT/HPC (43.3%) followed by ES (23.3%). In the series of 20 cases reported by Ghosal et al, metastasis was the most common tumor (30%) followed by SFT/HPC (25%).<sup>11</sup> ES/PNET (7 out of 30) could be attributed to the pediatric patients included in our study.

Spindle cell lesions and round blue cell tumors were the two broad categories encountered while evaluating nonmeningothelial dural-based lesions. The presence of stag-horn vessels along with spindle cells arranged in pattern-less architecture and hyalinized stroma pointed toward SFT/HPC. Nuclear features were evaluated to rule out pseudoinclusions of meningioma, especially fibrous variant. SFT/HPC showed

**Table 2** Diagnosis on magnetic resonance imaging and the respective histopathologic diagnosis of the cases in our study

MRI diagnosis	Histopathologic diagnosis
Meningioma (20)	SFT/HPC (9) ES (5) Undifferentiated sarcoma (1) Plasmacytoma (1) Metastasis (1) Granulocytic sarcoma (1) RDD (1) Inflammatory (1)
SFT/HPC (4)	SFT/HPC (2) ES (1) Metastasis (1)
Sarcoma (2)	SFT/HPC (2)
Schwannoma (2)	ES (1) NHL (1)
Inflammatory lesion (1)	Inflammatory (1)
Hemangioma (1)	RDD (1)

Abbreviations: ES, Ewing's sarcoma; HPC, hemangiopericytoma; MRI, magnetic resonance imaging; NHL, non-Hodgkin's lymphoma; RDD, Rosai–Dorfman disease; SFT, solitary fibrous tumor.  
Note: Parenthesis indicating the number of cases.

moderately dense nuclear chromatin with inconspicuous nucleoli. We reviewed our cases and graded the lesions as per the 2016 WHO classification of CNS tumors. Negativity for epithelial membrane antigen (EMA) and positive CD34 as well as Bcl2 IHC further aided to rule out meningioma. In view of small cells, mitosis and necrosis seen in Grade III lesions, anaplastic meningioma, ES/PNET, and malignant peripheral nerve sheath tumor needed to be ruled out.

Above-mentioned IHC markers along with negativity for S100p and CD99 helped to rule out these other lesions. Nuclear expression of signal transducer and activator of transcription (STAT) 6 indicative of NAB2-STAT6 fusion is now considered characteristic for SFT/HPC.<sup>12</sup> However, IHC for STAT 6 was not performed, due to lack of availability of the antibody at our institute.

One of our cases of SFT/HPC was located in the cervical spinal region, which is a rare finding. Less than 90 cases of intradural extramedullary SFT/HPC in the spinal region have been reported in the literature with thoracic region being the most common site.<sup>13</sup>

For the tumor labeled as undifferentiated sarcoma, even on extensive screening, we did not observe any pigment or HPC-like vasculature. Nuclei were hyperchromatic without the presence of prominent nucleoli. Areas of necrosis and brisk mitotic activity along with presence of bizarre cells were noted. The morphology was suggestive of a high-grade spindle cell tumor with brain invasion and the tumor did not show positivity for any of the specific IHC markers, as listed in **Table 1**.

Coming to the tumors with round blue cell morphology, differentials considered were ES/PNET, lymphomas, synovial sarcoma, rhabdomyosarcoma, and mesenchymal chondrosarcoma. Absence of rhabdoid-like cells and islands of mature-appearing hyaline cartilage helped rule out the latter two. The first panel of IHC markers for almost all cases comprised leucocyte common antigen (LCA), desmin, CD99, and AE1/AE3.

Diffuse and strong immunoreactivity for CD99 helped to diagnose ES/PNET. These are known to affect the calvarium and secondarily invade the dura, but are extremely rare as solitary dural lesions. Surgical excision followed by

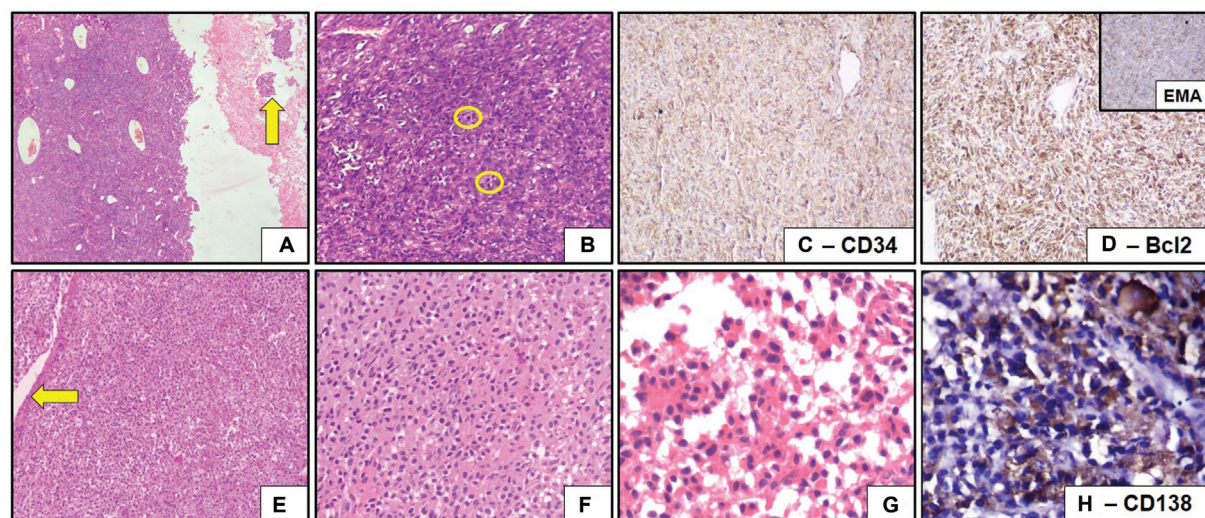


**Fig. 1** (A) Solitary fibrous tumor/hemangiopericytoma. Grade III—highly cellular tumor invading into the brain (yellow arrow). Dilated blood vessels seen amidst the haphazardly arranged tumor cells (hematoxylin and eosin [H and E],  $\times 100$ ). (B) High power view of tumor seen in (A) demonstrating spindle cells with moderate amount of eosinophilic cytoplasm and ovoid, hyperchromatic nuclei showing marked pleomorphism, atypical mitotic figures (yellow circles) (H and E,  $\times 400$ ). (C and D) Tumor cells showing positivity for CD34, Bcl2, inset: negative for epithelial membrane antigen (EMA) (representative images for the cases discussed) (immunohistochemistry [IHC],  $\times 100$ ). (E) Tumor composed of sheets of cells abutting the dura (yellow arrow) (H and E,  $\times 40$ ). (F) Cells arranged in sheets with hyperchromatic round to ovoid nuclei (H and E,  $\times 100$ ). (G) Individual cells are round to polygonal with eccentrically placed nuclei and abundant eosinophilic cytoplasm (H and E,  $\times 400$ ). (H) Tumor cells showing membranous positivity for CD138, confirming the lesion as plasmacytoma (IHC,  $\times 400$ ).

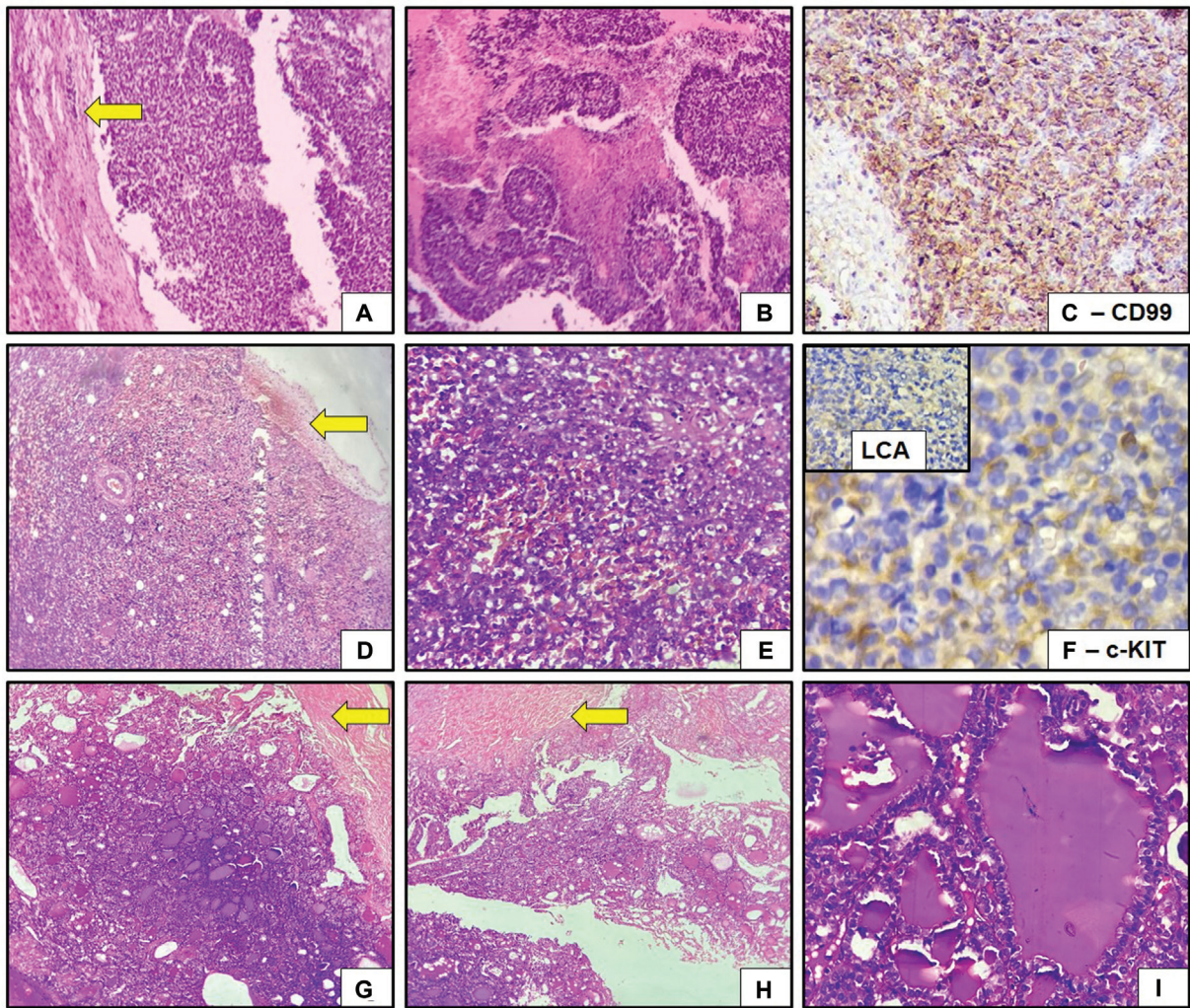


**Fig. 2** (A) Highly cellular tumor composed of round blue cells adjacent to the dura (*yellow arrow*) (hematoxylin and eosin [H and E],  $\times 100$ ). (B) Tumor showed presence of perivascular pseudorosettes and areas of necrosis (H and E,  $\times 100$ ). (C) Tumor cells are positive for CD99 helping to arrive at the diagnosis of Ewing's sarcoma (immunohistochemistry [IHC],  $\times 100$ ). (D) Dura (*yellow arrow*) with underlying tumor (H and E,  $\times 100$ ). (E) Individual tumor cells with round blue cell morphology, abundant mitotic figures (H and E,  $\times 400$ ). (F) Tumor cells showing positivity for c-KIT (CD117) (IHC,  $\times 400$ ). Inset showing negative staining for leucocyte common antigen (IHC,  $\times 400$ )—granulocytic sarcoma. (G and H) Tumor seen abutting the dura (*yellow arrow*). Tumor is composed of follicles (H and E,  $\times 100$ ). (I) Tumor composed of follicles lined by cuboidal epithelium and containing colloid, suggestive of metastasis of follicular carcinoma of thyroid (H and E,  $\times 400$ ).

chemoradiotherapy is the usual treatment protocol for these patients.<sup>3</sup> In our study, ES/PNET was the second most common lesion (23.3%) with two cases having an intradural extramedullary location in the lumbar region. On MRI, one

of the lesions was called as meningioma and the other as schwannoma, none of these showed bony involvement.

Another diagnostically challenging case was of ALCL. As reported by Iwamoto and Abrey in their review, dural

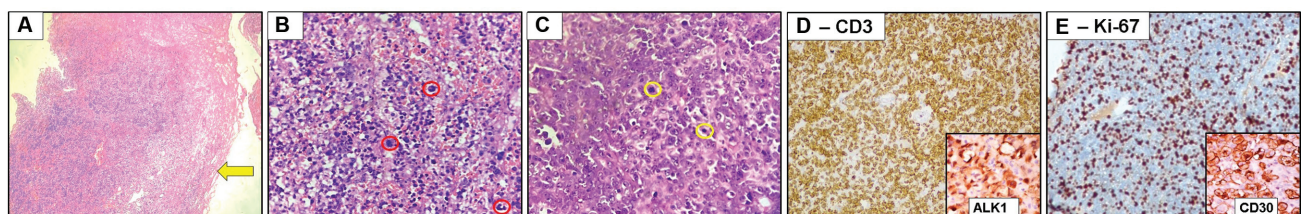


**Fig. 3** (A) Anaplastic large cell lymphoma. Highly cellular tumor seen abutting the dura (*yellow arrow*) (hematoxylin and eosin [H and E],  $\times 100$ ). (B) High power view showing the tumor is composed predominantly of lymphocytes. “Hallmark cells” seen (*red circles*) (H and E,  $\times 400$ ). (C) Atypical mitotic figures (*yellow circles*). (D) Tumor cells showed diffuse positivity for CD3, inset: positivity for anaplastic lymphoma kinase (ALK)-1 immunohistochemistry (IHC). (E) Ki-67 index  $\sim 80\%$ , inset: CD30 expressed by tumor cells.

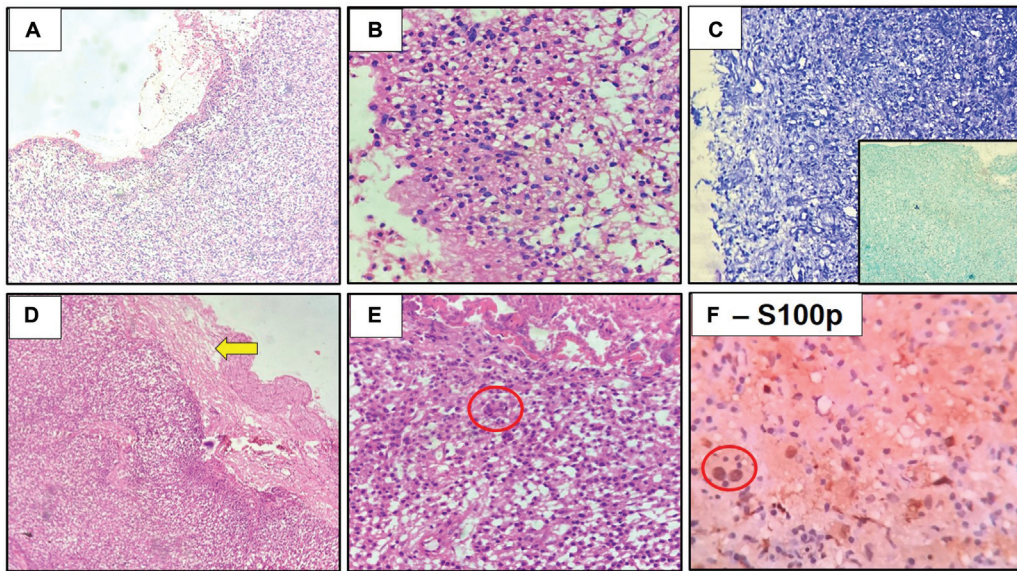


**Fig. 4** (A) Polymorphous population of cells seen beneath the dura (hematoxylin and eosin [H and E], ×100). (B) Lymphocytes and few foamy macrophages seen (H and E, ×400). (C) No acid fast bacilli seen on Ziehl-Neelsen staining (acid-fast bacilli [AFB], ×400), inset: no fungal organisms seen (Gomori methenamine silver stain, ×400)- non-specific inflammatory lesion. (D) Lesion seen adjacent to the dura (yellow arrow) (H and E, ×100). (E) High power view showing polymorphous population of inflammatory cells. Some of the cells show emperipolesis (macrophages with engulfed lymphocytes—red circle) (H and E, ×400). (F) Histiocytes with engulfed lymphocytes expressing S100p (red circle) - Rosai-Dorfman disease.

**Table 3** Prevalence and comparison of lesions seen in our study with that reported in the literature

Lesion	Prevalence	Age group		Sex predilection		Location	
		Literature	Our study	Literature	Our study	Literature	Our study
SFT/HPC	< 1% <sup>1,a</sup>	4th–5th decade <sup>2</sup>	3rd–5th decade	Males <sup>2</sup>	Male	Most supratentorial; 10% spinal <sup>2</sup>	Maximum intracranial, 1 case spinal
ES	< 50 cases <sup>3,a</sup>	2nd decade <sup>3</sup>	2nd decade	Males <sup>3</sup>	Male	Both supra- and infratentorial <sup>3</sup>	5 - supratentorial 2 - spinal
Metastasis	9–10% <sup>4,a</sup>	6th decade <sup>4</sup>	5th decade	Female <sup>4</sup>	Male	Supratentorial <sup>4</sup>	Supratentorial
ALCL, ALK positive	2 cases <sup>5,6,a</sup>	Young <sup>6</sup>	5th decade	Male <sup>6</sup>	Male	Intracranial <sup>6</sup>	Spinal
Plasmacytoma	< 20 cases <sup>7,a</sup>	Elderly <sup>7</sup>	6th decade	Female <sup>7</sup>	Female	Supratentorial <sup>7</sup>	Supratentorial
Granulocytic sarcoma	0.4–0.7% of AML patients <sup>8</sup>	Wide age range	1st decade	Equal <sup>8</sup>	Male	Supratentorial <sup>8</sup>	Thoracic spine
Undifferentiated sarcoma	< 40 cases <sup>9,a</sup>	All age groups <sup>9</sup>	3rd decade	Equal <sup>9</sup>	Male	Supratentorial <sup>9</sup>	Supratentorial - parasagittal
RDD	< 5% show CNS involvement <sup>10</sup>	4th decade <sup>10</sup>	4th and 5th decade	Male <sup>10</sup>	Equal	Intracranial <sup>10</sup>	1 - intracranial 1 - spinal

Abbreviations: ALCL, anaplastic large cell lymphoma; ALK, anaplastic lymphoma kinase; AML, acute myeloid leukemia; CNS, central nervous system; ES, Ewing’s sarcoma; HPC, hemangiopericytoma; RDD, Rosai-Dorfman disease; SFT, solitary fibrous tumor.

<sup>a</sup>For dural-based lesion.

lymphomas are mostly low-grade B cell marginal zone lymphomas.<sup>14</sup> Our case had large cell-type morphology with presence of multinucleated cells, “hallmark cells,” and showed diffuse positivity for CD3 indicating a T cell phenotype. Positivity for CD30 helped to clinch the diagnosis and ALK-1 helped to label it as ALCL, ALK-positive. Unfortunately, our patient expired on the fifth day postoperatively and further workup to look for lesions elsewhere could not be performed. Only two cases of dural-based T cell NHL have

been reported in the literature so far. Furthermore, none of these patients were immunosuppressed like ours.<sup>5,6</sup>

The other round blue cell tumor in our series was a granulocytic sarcoma. Patient being only 8 years old, an initial panel of LCA, CD99, and desmin was performed, after morphologic conclusion of a round blue cell tumor. The morphology was not suggestive of meningioma as suggested on MRI. Further probe into history of the patient unveiled him as being a known case of AML on treatment. This prompted us to

perform CD117 (c-KIT) IHC. Furthermore, granulocytic sarcomas are known to occur as soft-tissue masses in the spinal region but an intradural extramedullary location is reported in only a few case reports.<sup>15</sup> These occur as focal masses most commonly in the skin, bone, soft tissue, and lymph nodes while involvement of the CNS is rare and can form as a focal lesion within the brain or dura. Chemoradiotherapy is the treatment of choice.<sup>8</sup>

Solitary plasmacytoma in our study was mimicking meningioma on MRI. On microscopic examination, it showed sheets of cells with plasmacytoid morphology expressing positivity for CD38, CD138, and lambda light chain restriction. No invasion into the adjacent brain parenchyma was observed on both microscopy and radiology. Plasmablastic lymphoma was ruled out in view of negativity for LCA and CD20. Furthermore, our patient was not immunosuppressed. Plasmacytomas are again reported to occur as soft-tissue lesions and dural-based location has been reported in association with multiple myeloma. Further workup of the patient with whole-body positron emission tomography scan ruled out any systemic illness, thus confirming this to be a case of solitary extraosseous plasmacytoma. As mentioned above, solitary plasmacytomas of the dura are extremely rare, radiosensitive tumors, but the patient needs to be followed up on a regular basis to detect the development of any systemic illness at the earliest.<sup>7</sup>

Metastasis was the most commonly reported lesion in the series by Ghosal et al (30%),<sup>11</sup> while we observed only 6.7% such lesions. Dural seeding from metastatic deposits is commonly reported for breast and prostate carcinomas.<sup>4</sup> Very few case reports are available in the literature describing the metastasis of follicular carcinoma of thyroid to the dura, and these were associated with overlying osteolytic lesions of the skull.<sup>16,17</sup> With the clinical history and classic morphology comprising of follicles lined by cuboidal cells, some showing presence of colloid we could arrive at the diagnosis. The lesion was located in the parietal region without involvement of overlying skull bone. For the other metastatic lesion, other than AE1/AE3, an extensive panel of IHC markers was negative. The patient expired on the second day postoperatively and further workup could not be performed to locate the primary. Hence, the tumor was labeled as undifferentiated metastatic carcinoma, with unknown primary.

CNS involvement by RDD is seen in less than 5% of the cases and is usually associated with nodal disease elsewhere in the body.<sup>10</sup> Unfortunately, clinical details were not available for our patients. On morphology, differentials considered were inflammatory lesion secondary to an infectious process, lymphoplasmacyte-rich meningioma, and Erdheim–Chester disease. The characteristic feature of emperipolesis helped to clinch the diagnosis. Besides this, special stains to detect any organisms were negative, the histiocytes were positive for S100p and IHC for CD1a, EMA were negative, ruling out the other possibilities. For intracranial lesions, RDD has been reported in the parasellar region, parietal convexity, and cerebellopontine angle, to name a few and 14% lesions have been reported to occur in the spine.<sup>18</sup>

The inflammatory lesions in our study were not diagnostic of any specific etiology, but presented as space-occupying lesions on radiology (►Table 2). In both the cases, we observed a mixed inflammatory infiltrate comprising lymphocytes, plasma cells, few histiocytes, and neutrophils. No granuloma formation, giant cells, or caseous necrosis was seen. Special stains for both acid fast bacilli and fungi were negative. However, the patients responded well to surgery and antibiotic treatment. Inflammatory lesions of the dura are mostly attributable to either tuberculosis, sarcoidosis, or fungal granuloma formation. Based on morphology, these were ruled out in our case. The cause of these in our study forming a mass-like lesion remains unknown.

There was discrepancy between the radiologic findings and the histopathologic diagnosis as shown in ►Table 2, with 66.7% of the lesions called as meningioma on MRI. Similarly, meningioma was the diagnosis for all 20 lesions reported by Ghosal et al.<sup>11</sup> The “dural-tail sign” which has been considered as specific for meningioma is also reported with other lesions such as neuromas, metastases, granulocytic sarcoma, lymphoma, granulomatous disorders, and cerebral Erdheim–Chester disease.<sup>19</sup> Besides this, “volcano sign,” which indicates a focal break in the dural lining, can be used by radiologists to diagnose a rapidly growing, aggressive dural neoplasm.<sup>20</sup>

However, radiologic diagnosis has its limitations, so pathologic examination of the tissue remains the gold standard to rule out meningioma and to establish the diagnosis as well as to grade the tumors to guide accurate therapeutic decisions.

Although we observed and discussed the rare lesions affecting the dura, some of the other lesions that have to be borne in mind, while diagnosing nonmeningothelial dural-based masses are neurosarcoidosis, melanomas, hemangiomas, hemangioendotheliomas, and the sarcomas listed above.

Lack of availability of follow-up data was a limitation of our study. However, with this study, we have tried to discuss some of the practical challenges in diagnosing nonmeningothelial tumors in view of their rarity as well as overlapping clinicopathological features. As always, a combined approach with clinical and radiologic details, aids to arrive at the diagnosis.

## Conclusion

Occurrence of dural-based lesions, besides meningioma is rare. Diagnosis requires thorough assessment of the morphological features which may guide the employment of ancillary tests such as IHC to rule out differentials. Accurate diagnosis is a must since all of these have different treatment protocols and prognosis.

### Authors' Contribution

P.K.G. contributed to the concept, design, definition of intellectual content, literature search, experimental studies, data acquisition, data analysis, manuscript preparation, manuscript editing, and manuscript review. A.S.S.

contributed to the concept, design, definition of intellectual content, literature search, data acquisition, manuscript preparation, manuscript editing, and manuscript review. She is also the guarantor for the paper. N.A.G. contributed to the concept, definition of intellectual content, literature research, manuscript editing, and manuscript review.

#### Conflict of Interest

None declared.

#### References

- 1 Brat DJ, Perry A, Wesseling P, Bastian BC. Melanocytic tumors. In: Louis DN, ed. WHO Classification of Tumours of the Central Nervous System. Revised 4th ed. Lyon: IARC; 2016:247–264
- 2 Damodaran O, Robbins P, Knuckey N, Bynevelt M, Wong G, Lee G. Primary intracranial haemangiopericytoma: comparison of survival outcomes and metastatic potential in WHO grade II and III variants. *J Clin Neurosci* 2014;21(08):1310–1314
- 3 Panagopoulos D, Themistocleous M, Apostolopoulou K, Sfakianos G. Primary, dural-based, Ewing sarcoma manifesting with seizure activity: presentation of a rare tumor entity with literature review. *World Neurosurg* 2019;129:216–220
- 4 Nayak L, Abrey LE, Iwamoto FM. Intracranial dural metastases. *Cancer* 2009;115(09):1947–1953
- 5 Kaku MV, Savardekar AR, Muthane Y, Arivazhagan A, Rao MB. Primary central nervous system dural-based anaplastic large cell lymphoma: diagnostic considerations, prognostic factors, and treatment modalities. *Neurol India* 2017;65(02):402–405
- 6 Kim MK, Cho CH, Sung WJ, et al. Primary anaplastic large cell lymphoma in the dura of the brain: case report and prediction of a favorable prognosis. *Int J Clin Exp Pathol* 2013;6(08):1643–1651
- 7 Azarpira N, Noshadi P, Pakbaz S, Torabineghad S, Rakei M, Safai A. Dural plasmacytoma mimicking meningioma. *Turk Neurosurg* 2014;24(03):403–405
- 8 Cervantes GM, Cayci Z. Intracranial CNS manifestations of myeloid sarcoma in patients with acute myeloid leukemia: review of the literature and three case reports from the author's institution. *J Clin Med* 2015;4(05):1102–1112
- 9 Wapshott T, Schammel CMG, Schammel DP, Rezeanu L, Lynn M. Primary undifferentiated sarcoma of the meninges: a case report and comprehensive review of the literature. *J Clin Neurosci* 2018; 54:128–135
- 10 Wen JH, Wang C, Jin YY, et al. Radiological and clinical findings of isolated meningeal Rosai-Dorfman disease of the central nervous system. *Medicine (Baltimore)* 2019;98(19):e15365
- 11 Ghosal N, Dadlani R, Gupta K, Furtado SV, Hegde AS. A clinicopathological study of diagnostically challenging meningioma mimics. *J Neurooncol* 2012;106(02):339–352
- 12 Chmielecki J, Crago AM, Rosenberg M, et al. Whole-exome sequencing identifies a recurrent NAB2-STAT6 fusion in solitary fibrous tumors. *Nat Genet* 2013;45(02):131–132
- 13 Tomomatsu Y, Iizuka Y, Mieda T, et al. Intradural-extramedullary solitary fibrous tumor/hemangiopericytoma with a negative result on fluorodeoxyglucose-positron emission tomography/computed tomography. *Case Rep Orthop* 2019:3926903
- 14 Iwamoto FM, Abrey LE. Primary dural lymphomas: a review. *Neurosurg Focus* 2006;21(05):E5
- 15 Mosch A, Kuiters RR, Kazzaz BA. Intradural granulocytic sarcoma: a rare cause of sciatic pain. *Clin Neurol Neurosurg* 1991;93(04): 341–344
- 16 Tazi M, Essadi I, Errihani H. Thyroid carcinoma presenting as a dural metastasis mimicking a meningioma: a case report. *N Am J Med Sci* 2011;3(01):39–42
- 17 Arora D, Singh N, Doda V. Lytic skull metastasis from follicular carcinoma of thyroid: a case diagnosed on cytology. *J Family Community Med* 2018;25(02):129–130
- 18 Adeleye AO, Amir G, Fraifeld S, Shoshan Y, Umansky F, Spektor S. Diagnosis and management of Rosai-Dorfman disease involving the central nervous system. *Neurol Res* 2010;32(06): 572–578
- 19 Guermazi A, Lafitte F, Miaux Y, Adem C, Bonneville JF, Chiras J. The dural tail sign—beyond meningioma. *Clin Radiol* 2005;60(02): 171–188
- 20 Prabhu SP. “Volcano sign”—description of a sign of aggressive neoplastic epidural lesions with subdural extension. *Childs Nerv Syst* 2009;25(04):399–402